Adsorption behavior and practical separation of some radionuclides using cellulose/HO$_7$Sb$_3$

Sara S. Mahrous[a],*, E. A. Abdel-Galil[a], N. Belacy[a], Ebtissam A. Saad[b]

[a]Environmental Radioactive Pollution Department, Hot Laboratories Center, Atomic Energy Authority, P.O. Box 13759, Cairo, Egypt, Tel. +20 1099205501; Fax: +20 244620784; email: drsaramahrous.eaea@yahoo.com (S.S. Mahrous), Tel. +20 1110937040; Fax: +20 244620784; email: ezzat_20010@yahoo.com (E. A. Abdel-Galil), Tel. +20 1002586225; Fax: +20 244620784; email: nabil_belacy@yahoo.com (N. Belacy)
[b]Faculty of Science, Ain Shams University, Cairo, Egypt, Tel. +20 1119107130; email: ebtissamsaad@yahoo.com

ABSTRACT

Testing and evaluation of sorption kinetics, isotherms, and thermodynamics for cellulose/HO$_7$Sb$_3$ nanocomposite surface were demonstrated. Saturation capacity of La^{3+}, Co^{2+}, and Cs$^+$ onto cellulose/HO$_7$Sb$_3$ nanocomposite was calculated at different pH and initial metal concentrations. Kinetic (pseudo-first-order, pseudo-second-order, and intraparticle diffusion) and isotherm (Langmuir, Freundlich, and Dubinin–Radushkevich [D–R]) models were applied to the prepared nanocomposite. Kinetic data are well fitted with pseudo-second-order kinetic model. From Dubinin–Radushkevich isotherm model, the sorption process is controlled by chemical adsorption for both La^{3+} and Co^{2+}, while for Cs$^+$ is controlled by physical adsorption. According to the value of adsorption capacities, cellulose/HO$_7$Sb$_3$ seems to be a better sorbent for La^{3+} than Co^{2+} and Cs$^+$ with high removal efficiency for the studied metal ions. Separation of La^{3+} ions using chromatographic column packed with cellulose/HO$_7$Sb$_3$ was achieved successfully.

Keywords: Cellulose/HO$_7$Sb$_3$; Capacity; Kinetic model; Adsorption isotherm; Separation

1. Introduction

Low-level radioactive liquid wastes (LLW) are increasing everyday according to nuclear technology expansion. There are different techniques for the treatment of liquid radioactive waste, for example, ion exchange [1–4], solvent extraction [5], biodegradation, and adsorption techniques [6]. Adsorption technique is preferred than the others because of its simplicity and affordability.

Organic and inorganic materials are the basis of this technique; however, organic sorbents exhibit large capacity with low radiation stability. Impregnation is one of the favored techniques to improve the properties of the organic sorbents, increasing their sorption capacity, selectivity, radiation stability, and uniformity. Different organic substances are commonly utilized for the sorption process such as polysaccharides (Alginic acid and cellulose), proteins (keratin, casein, and collagen), and carbonaceous materials (e.g., charcoals).

When designing an adsorbing composite, it is better to predict the rate at which the reaction will occur. Calculation of the equilibrium adsorption data can be done by many approaches, for example, Langmuir, Freundlich, and Dubinin–Radushkevich (D–R) isotherm models. Monolayer formation of adsorbed metal ion on the adsorbent surface can be discussed by Langmuir isotherm model. Freundlich isotherm model is used to explain the adsorption characteristics for the heterogeneous surface, while Dubinin–Radushkevich isotherm model is discussing the mechanism of energy distribution on a heterogeneous surface with Gaussian energy distribution.

* Corresponding author.

Thermodynamic parameters such as standard enthalpy change ($\Delta H°$), standard entropy change ($\Delta S°$), and standard Gibbs free energy change ($\Delta G°$) should be calculated to indicate adsorption reaction type using equilibrium constant values at various temperatures.

It is important to recognize the adsorption kinetics, which defines the possible mechanism of metal ion transfer from the bulk solution to the adsorbent surface. Sorption kinetics is conducted through the next procedures: (a) transference of solute in the bulk of the solution; (b) diffusion of solute across the liquid film which surrounds the sorbent particles; (c) flow of solute in the liquid contained in the pores of adsorbent particle and along the pore walls (intraparticle diffusion); (d) adsorption and desorption of solute, for example, (adsorbate metal ions) on/from the sorbent surface. To analyze the kinetic sorption process, pseudo-first, second-order, and diffusion-based models were applied [7].

The present study concerns the investigation of both kinetic and isotherm models for the prepared sorbent cellulose/HO$_7$Sb$_3$, in addition, testing the efficiency of the prepared composite in the removal of the studied metal ions by column experiment. Finally, the conditions for the regeneration process has been obtained for the reuse of the prepared composite

2. Experimental

2.1. Reagents

The chemicals used for the preparation of the sorbent material were obtained from BDH (England) and Loba Chemie (India). All supplementary reagents and chemicals are of analytical grade purity and used without any further purification. Metal ion solutions of different concentrations were prepared from their pure metal salts.

2.2. Sorbent preparation and characterization

Cellulose/HO$_7$Sb$_3$ composite was previously prepared and characterized by Abdel-Galil et al. [8].

2.3. Capacity measurements

Capacity of cellulose/HO$_7$Sb$_3$ was measured for La^{3+}, Co^{2+}, and Cs$^+$ ions with repeated batch technique in different metal ion concentrations (100 to 800 mg L^{-1}) and different solution pH values (1 to 6.5) at V/m = 100 mL g^{-1}. The mixture was shaken in a thermostatic shaker (Kottermann D-1362, Germany) at 400 rpm at 25±1°C for 2 hr until equilibrium reached [8]. After solid separation, the residual concentration of La^{3+}, Co^{2+} ions were measured with inductive coupled plasma (ICP) spectrophotometer, while the residual concentration of Cs$^+$ ions was measured with atomic absorption spectrophotometer (AAS). Saturation capacity (mg g^{-1}) was calculated as follows:

$$\text{Capacity}\left(\text{mg/g}\right) = \left(\frac{\% \text{ uptake}}{100}\right) \times C_0 \times \frac{V}{m} \tag{1}$$

in which C_0 is the initial concentration of the metal ion in mg L^{-1}, V is the volume of the solution in L, and m is th mass in g.

2.4. Kinetic experiments

Kinetic experiments were done by adding 5 mL of metal ion solution of 50 mg L^{-1} to 0.05 g of prepared composite at a V/m ratio of 100 mL g^{-1} and different temperatures (298, 318, and 338 K) and shaking speed of 400 rpm using a thermostatic shaker. Samples were taken from the shaker at preset time (5–300 min). To avoid colloidal suspension, the sorbents were filtered from the solution through 0.454 μm filter paper. The concentration of La^{3+}, Co^{2+}, and Cs$^+$ ions was measured in the supernatant, while the adsorption capacity at equilibrium, q_e (mg g^{-1}) was calculated.

2.5. Adsorption isotherm experiments

Adsorption isotherms of La^{3+}, Co^{2+}, and Cs$^+$ ions in the presence of cellulose/HO$_7$Sb$_3$ were conducted for 5 mL solutions added to 0.05 g sorbent at V/m = 100 mL g^{-1}. The adsorption isotherms for the selected ions were measured at different concentrations (50–400 mg L^{-1}). The mixture was shaken for 2 hr at different temperatures (298, 318, and 338 K) in a shaker bath. After equilibrium, solutions were filtered using filter paper. The concentration of La^{3+}, Co^{2+}, and Cs$^+$ ions was measured instrumentally as shown above. All tests were repeated for three times to reduce the error percent; the estimated error was about ±3%.

2.6. Continuous flow experiment

Chromatographic column breakthrough examination was achieved in this manner; 1 g of the cellulose/HO$_7$Sb$_3$ of particle size <100 μm was packed in a glass column (1.4 cm diameter and 5 cm height) to give a bed height of 2.2 cm^3 volume. Volume of 400 mL of the desired neutral solutions (pH = 5.5 (containing 100 mg L^{-1} of the metal chloride [M(Cl)$_X$ where, M = La^{3+}, Co^{2+}, and Cs$^+$])) was passed through the column beds at a flow rate of 5–6 drop min^{-1}. Equal portions were collected and the concentration was measured by using ICP spectrophotometer and AAS. Breakthrough capacity values can be estimated as:

$$\text{Breakthrough capacity}\left(\text{mg/g}\right) = V_{(50\%)} \times \frac{C_i}{m} \tag{2}$$

where $V_{(50\%)}$ is the effluent volume at 50% breakthrough in mL, C_i is the concentration of feed solution in mg L^{-1}, and m is the amount of the column bed in g.

3. Results and discussion

3.1. Saturation capacity

Saturation capacity of La^{3+}, Co^{2+}, and Cs$^+$ ions onto cellulose/HO$_7$Sb$_3$ composite was measured experimentally via repeated batch sorption technique.

The capacity of cellulose/HO$_7$Sb$_3$ for the studied metal ions at different concentrations is summarized in Table 1. It is clear that the capacity of cellulose/HO$_7$Sb$_3$ for La^{3+}, Co^{2+}, and Cs$^+$ ions increased as the initial concentrations of metal ions raised from 100 to 800 mg L^{-1}. In the concentration range between 100 and 400 mg L^{-1}), the capacity of the prepared composite for La^{3+}, Co^{2+}, and Cs$^+$ ions was greatly increased.

Table 1
Cellulose/HO$_7$Sb$_3$ capacity of the studied metal ions at different concentrations

Concentration (mg L⁻¹)	Capacity (mg g⁻¹)		
	La³⁺	Co²⁺	Cs⁺
100	21.27	17.33	16.00
200	35.46	31.09	25.50
300	60.00	40.50	30.90
400	82.46	52.80	35.50
600	88.26	55.50	44.20
800	91.80	55.90	45.85

On the other hand, at high concentrations 600–800 mg L⁻¹ slight increase in the capacity was observed. At low concentrations, the active sites were available for quick binding. At higher concentrations, the binding sites available for adsorption decreased and hence slow diffusion of the studied metal ions to the nanocomposite surface occurred [9]. It was found that the capacity of cellulose/HO$_7$Sb$_3$ for the studied metal ions takes the order; La³⁺ > Co²⁺ > Cs⁺. This sequence is in accordance with the ionic radii of the sorbed ions; the ions with smaller ionic radii are easily adsorbed and move faster than those with greater ionic radii [8,10]. In addition, multivalent ions possess a greater complexing ability than the mono and divalent one [11]. El-Naggar et al. [12,13] report similar conclusion. Cellulose/HO$_7$Sb$_3$ capacity for La³⁺, Co²⁺, and Cs⁺ ions was determined as a function of pH at a constant concentration (800 mg L⁻¹) of the metal ions. The data obtained are recorded in Table 2. The data show that the capacity of cellulose/HO$_7$Sb$_3$ for the studied metal ions increases with increasing the pH of the solution. This may be due to the decrease of the [H]⁺ in solution that facilitates the release of H⁺ from the surface of composite in solution and this stimulates the adsorption process. Therefore, by increasing the percent uptake of the metal ions, the capacity consequently increases [6].

3.2. Sorption kinetics

To determine the kinetics of the sorption process and investigate the mechanism of metal ions sorption, two different sorption kinetic models were applied; reaction-based models and diffusion-based models [14].

Table 2
Cellulose/HO$_7$Sb$_3$ capacity of the studied metal ions at different pH values and constant concentration (800 mg L⁻¹)

pH	Capacity (mg g⁻¹)		
	La³⁺	Co²⁺	Cs⁺
1	19.33	17.10	14.80
2	26.68	23.70	19.10
3	55.50	45.80	33.60
4	86.70	50.20	40.50
5.5	91.80	55.90	45.85

3.2.1. Reaction-based models

3.2.1.1. Pseudo-first-order

Lagergren [15] proposed a method for adsorption analysis in which the pseudo-first-order kinetic equation is given as:

$$\ln\left(q_e - q_t\right) = \ln q_e - k_1 t \tag{3}$$

where q_e and q_t (mg g⁻¹) are the adsorbed quantity of ions per sorbent unit mass at equilibrium and at any time, t, respectively, and k_1 is the pseudo-first-order rate constant in g mg⁻¹ min⁻¹. By plotting ln ($q_e - q_t$) vs. t, straight lines are obtained as shown in Fig. 1(a). The values of pseudo-first-order rate constants, k_1, and equilibrium adsorption capacities, q_e, can be acquired from the slope and intercept, respectively. The parameters of pseudo-first-order model and the linear regression correlation coefficient R^2 are summarized in Table 3.

3.2.1.2. Pseudo-second-order

The second-model used to describe the sorption of La³⁺, Co²⁺, and Cs⁺ on cellulose/HO$_7$Sb$_3$ is pseudo-second-order kinetic model. It is given in [16,17] as:

$$\frac{t}{q_t} = \frac{1}{k_2 q_e^2} + \frac{t}{q_e} \tag{4}$$

Both q_e and k_2 are calculated from the slope and intercept of the plots t/q_t versus t, respectively as shown in Fig. 1(b). The constant k_2 is used to calculate the initial sorption rate h (mg g⁻¹ min⁻¹), as $t \rightarrow 0$ as follows:

$$h = k_2 q_e^2 \tag{5}$$

where k_2 (g mg⁻¹ min⁻¹) is the pseudo-second-order rate constant, q_e is the adsorption capacity at equilibrium and q_t is the adsorption capacity at time t.

Pseudo-second-order rate constants k_2, the calculated h values, and the corresponding linear regression correlation coefficients R^2 are given in Table 3. According to the correlation coefficient (R^2) values in the two models, 0.998, 0.998, and 0.997 for La³⁺, Co²⁺, and Cs⁺, respectively, in pseudo-second-order model and 0.889, 0.854, and 0.918 for La³⁺, Co²⁺, and Cs⁺, respectively, in the pseudo-first-order model, it is clear that the kinetic data are fitted well by pseudo-second-order model. Moreover, the difference between the calculated and measured q_e is very small for pseudo-second-order model; however, the difference is large in the pseudo-first-order model [18]. From the above results, it is concluded that the sorption process of La³⁺, Co²⁺, and Cs⁺ ions from aqueous solution using cellulose/HO$_7$Sb$_3$ can be interpreted using pseudo-second-order model.

The half-adsorption time ($t_{1/2}$) is the time required to uptake half of the maximal amount of adsorbate at equilibrium [18], it is given as:
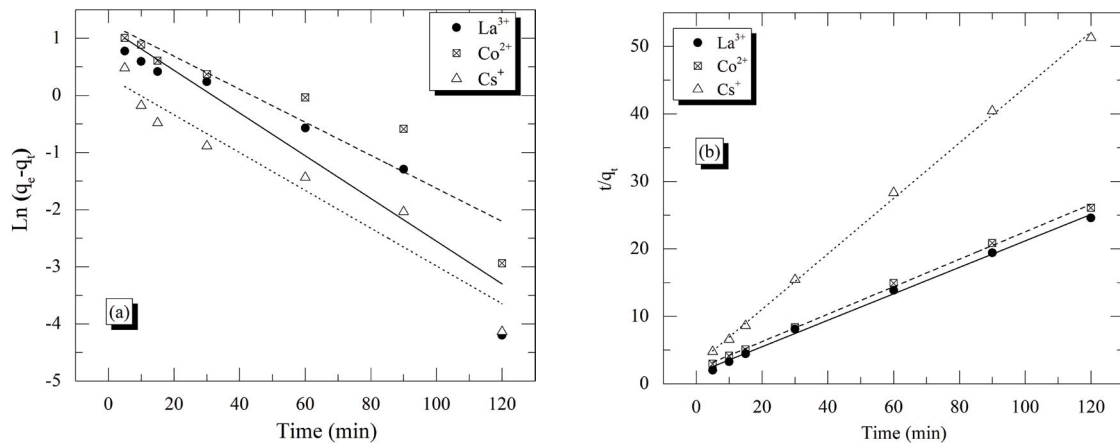
$$t_{1/2} = \frac{1}{k_2 \times q_e} \tag{6}$$

Fig. 1. Pseudo-first and pseudo-second-order kinetic for adsorption of La³⁺, Co²⁺, and Cs⁺ ions on cellulose/HO₇Sb₃ at 298 K.

Table 3
Adsorption rate constants, estimated q_e and coefficients of correlation associated for La³⁺, Co²⁺, and Cs⁺ ions according to the pseudo-first and pseudo-second-order kinetic models

| Cation | Temp. (K) | q_e(exp) (mg g⁻¹) | Pseudo-first-order | | | | Pseudo-second-order | | | | | |
			k_1 (g mg⁻¹ min⁻¹)	q_e (mg g⁻¹)	R^2	SD	k_2 (g mg⁻¹ min⁻¹)	q_e (mg g⁻¹)	h (mg g⁻¹ min⁻¹)	R^2	SD	$t_{1/2}$ (min)
La³⁺	298	4.99	0.037	3.27	0.89	0.633	0.022	5.17	0.596	0.998	0.003	8.66
Co²⁺	298	4.78	0.029	3.53	0.854	0.004	0.010	4.90	0.454	0.998	0.004	10.77
Cs⁺	298	2.35	0.033	1.30	0.918	0.004	0.042	2.47	0.290	0.997	0.008	8.52

The values of $t_{1/2}$ were decreased from 8.66 to 1.86, 10.77 to 2.69, and 8.52 to 7.66 for La³⁺, Co²⁺, and Cs⁺, respectively, as the reaction temperature increased from 298 to 338 K.

The activation energy of metal ion sorption was calculated from the pseudo-second-order constants (k_2) by the Arrhenius equation [19,20].

$$\ln(k_2) = \ln(A^\circ) - \frac{E_a}{RT} \qquad (7)$$

where E_a is the activation energy in kJ mol⁻¹, T is the temperature in K, and R is the gas constant (8.314 J mol⁻¹ K⁻¹), and A° is the temperature independent Arrhenius constant called the frequency factor. A linear relationship was obtained between $\ln(k_2)$ and $1/T$ as shown in Fig. 2.

From the slope of the linear plot, the activation energy for the adsorption of La³⁺, Co²⁺, and Cs⁺ ions on cellulose/HO₇Sb₃ was calculated and it was found to be 43.30, 29.37, and 16.00 kJ mol⁻¹ for La³⁺, Co²⁺, and Cs⁺ respectively, and the correlation coefficients are higher than 0.99. The positive values of E_a indicate that rise in temperature favors the adsorption and the adsorption process is an endothermic process [18].

3.2.2. Diffusion-based models

To illustrate the intraparticular diffusion of the system, the relationship between specific sorption (q_t) and the square root of time ($t^{1/2}$) was evaluated based on the following expression [21]:
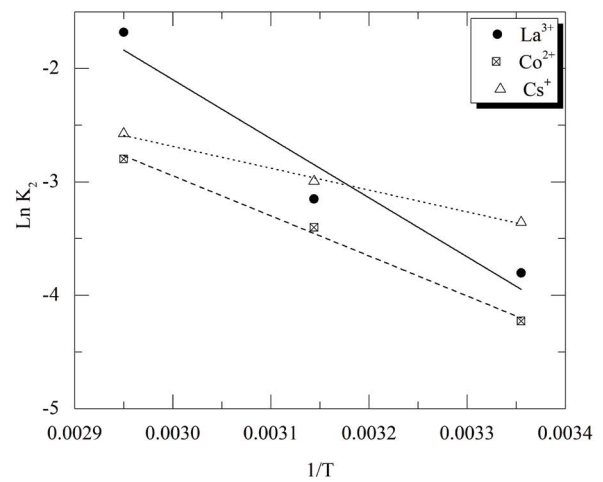

Fig. 2. Plots of $\ln k_2$ against reciprocal temperature of La³⁺, Co²⁺, and Cs⁺ ions on Cellulose/HO₇Sb₃.

$$q_t = K_{id}t^{1/2} + C \qquad (8)$$

where q_t (mg g⁻¹) is the amount of metal ions sorbed at time t (min), K_{id} is the intraparticle diffusion rate constant, and C is a constant. When mixing metal ion solution with adsorbent, metal ions transfer from the solution through liquid film between the solution and the adsorbent occurs into the pores inside the particles.

The intraparticle diffusion plotted in Fig. 3 shows multi-linearity in the diffusion of the La^{3+}, Co^{2+}, and Cs^+ ions within cellulose/HO_7Sb_3 as a function of time. The intraparticle diffusion model shows that the sorption process of La^{3+}, Co^{2+}, and Cs^+ occurs in three stages. The first stage is attributed to the diffusion of ions from the solution to the outer surface of the adsorbent. The second stage defines the regular sorption, where intraparticle diffusion is rate limiting and the third stage is caused by the final equilibrium due to extremely low sorbate concentration remained in the solution and the reduction of interior active sites [22]. The intraparticle diffusion constants for the three stages ($K_{id}1$, $K_{id}2$, and $K_{id}3$) are given in Table 4.

When the line passes through the origin ($C = 0$), the intraparticle diffusion will be the only rate control step [18,23]. If the line does not pass through the origin, this implies that intraparticle diffusion is not the exclusive rate control step but also other processes may control the rate of sorption [18].

3.3. Adsorption isotherms

In order to evaluate the nature of the sorption process of La^{3+}, Co^{2+}, and Cs^+ ions on cellulose/HO_7Sb_3 whether it is physical or chemical, the Langmuir, Freundlich, and Dubinin–Radushkevich (D–R) models were applied.

- The Langmuir model suggests that there is no interaction between metal ions after being adsorbed on a homogenous monolayer form on the adsorbent surface [24]. By plotting of C_e/q_e vs. C_e, it gives linear relationship, in which C_e is the equilibrium concentration of the adsorbate ions, q_e is the amount of ions adsorbed per gram of sorbent (mg g^{-1}) at equilibrium. The Langmuir constants Q and b were obtained from the slope and intercept of the linear plot, respectively, Fig. 4(a), and are summarized in Table 5. Based on the adsorption capacities, cellulose/HO_7Sb_3 seems to be a better sorbent for La^{3+} than the other studied cations.
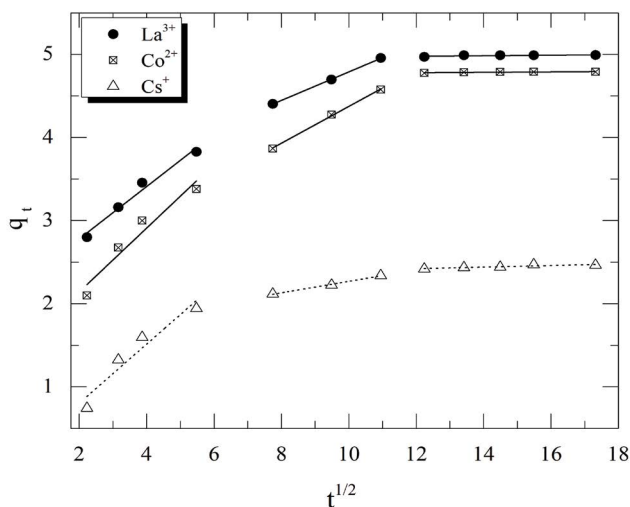
Fig. 3. Intraparticle diffusion kinetics for adsorption of La^{3+}, Co^{2+}, and Cs^+ ions on cellulose/HO_7Sb_3.

Table 4
Changes in the values of the intraparticular diffusion coefficients for La^{3+}, Co^{2+}, and Cs^+ ions

Cation	Intraparticle diffusion rate constant (K_{id})		
	First stage ($K_{id}1$)	Second stage ($K_{id}2$)	Third stage ($K_{id}3$)
La^{3+}	0.314	0.171	0.003
Co^{2+}	0.387	0.221	0.002
Cs^+	0.335	0.069	0.009

- Freundlich isotherm [25] was used to describe characteristics for the heterogeneous surface, reversible and non-ideality, of adsorption process regardless the creation of monolayer. This empirical model is applied for multilayer adsorption, with non-uniform distribution of adsorption heat and affinities over the heterogeneous surface. Plotting the log value of q_e vs. $logC_e$ generates a linear relationship, with a slope of $1/n$ and an intercept equal to log K_f as shown in Fig. 4(b). Here, $1/n$ ranges between 0 and 1 is a measure of the adsorption intensity or surface heterogeneity, and K_f (mg g^{-1}) is the adsorption capacity of the studied sorbent. The corresponding value of K_f and $1/n$ together with the correlation coefficients (R^2) are listed in Table 5.
- Dubinin–Radushkevich isotherm was applied to express the adsorption mechanism with a Gaussian energy distribution onto a heterogeneous surface [26]. Fig. 4(c) shows the plot of ln q_e vs. ε^2, gives a straight line with slope of $-K'$ and an intercept of ln X'_m. Where ε is the Polanyi potential $= RT \ln(1 + 1/C_e)$, X'_m is the adsorption capacity of the sorbent in mg g^{-1}, and K' is a constant related to the adsorption energy in mol^2 kJ^{-2}. The regression parameters and correlation coefficient (R^2) are listed in Table 5. This approach is usually applied to differentiate between the physical and chemical adsorption of metal ions with its mean free energy, E per molecule of adsorbate for eliminating adsorbed metal ions from its location in the sorption space to the infinity. It can be calculated by the following equation:

$$E = \left(-2K'\right)^{-1/2} \tag{9}$$

If ($E < 8$ kJ mol^{-1}), the sorption mechanism is physical. If ($8 < E < 16$ kJ mol^{-1}), the sorption is governed by ion exchange. If ($16 < E < 40$ kJ mol^{-1}), the sorption process is controlled by chemical adsorption process [4].

The correlation coefficient (R^2) determined from Langmuir isotherm for the La^{3+} and Co^{2+} is greater than that determined from Freundlich and D–R isotherm. In addition, it was found that $E = 59$ and 20 kJ mol^{-1} for La^{3+} and Co^{2+}, respectively, this confirms that the sorption of La^{3+} and Co^{2+} is governed by chemical adsorption. On the other hand, the calculated value of R^2 obtained from Freundlich isotherm for Cs^+ is greater than that obtained from Langmuir and D–R isotherm. Furthermore, the calculated value of $E < 8$ kJ mol^{-1}, confirms that the sorption of Cs^+ ions on cellulose/HO_7Sb_3 is physical adsorption.
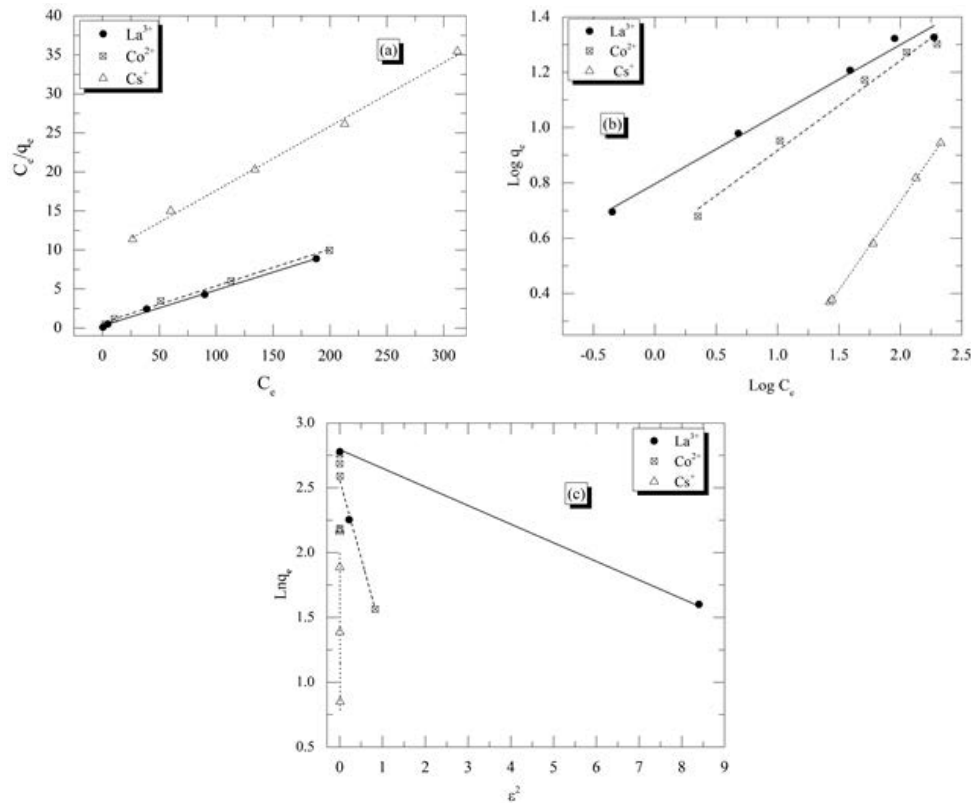
Fig. 4. Langmuir, Freundlich, and D–R adsorption isotherms for the adsorption of La^{3+}, Co^{2+}, and Cs^+ ions on cellulose/HO_7Sb_3.

Table 5
Isotherm models and calculated parameters for adsorption of La^{3+}, Co^{2+}, and Cs^+ ions on cellulose/HO_7Sb_3 at reaction temperature = 298 K

Isotherm model	Parameters	La^{3+}	Co^{2+}	Cs^+
Langmuir	Q_{max} (mg g^{-1})	21.86	21.21	14.31
	b (L mg^{-1})	0.159	0.071	0.005
	R^2	0.998	0.997	0.978
	R_L	0.015	0.34	0.333
Freundlich	$1/n$	0.251	0.324	0.603
	k_f (mg g^{-1})	6.25	3.90	3.03
	R^2	0.994	0.993	0.999
Dubinin–Radushkevich	X'_m (mg g^{-1})	16.34	12.91	7.80
	K' (mol^2 kJ^{-2})	0.143	1.20	1.54E-4
	E (kJ mol^{-1})	59.0	20.41	1.80
	R^2	0.662	0.737	0.784

The thermodynamic parameters were evaluated using Van't Hoff equation and the standard enthalpy change $\Delta H°$, standard Gibbs free energy change $\Delta G°$, and standard entropy change $\Delta S°$ are determined using Eqs. (10)–(13) [27,28]:

$$\Delta G° = -RT \ln\left(K_c\right) \tag{10}$$

$$K_c = Q_{max} b \tag{11}$$

$$\ln\left(K_c\right) = \frac{\Delta S°}{R} - \frac{\Delta H°}{RT} \tag{12}$$

$$\Delta G° = -nRT \tag{13}$$

where K_c (L g^{-1}) is the sorption equilibrium constant, R is the gas constant (8.314 J mol^{-1} K^{-1}), and T is the absolute temperature (K), and n represents the Freundlich constant. The values of enthalpy change ($\Delta H°$) and entropy change ($\Delta S°$) are presented for La^{3+} and Co^{2+} in Fig. 5(a) and for Cs^+ in Fig. 5(b). The obtained results are given in Table 6.

The positive value of $\Delta S°$ confirms that there is an increase in the randomness on the solid/solution interface during the sorption process. This result can be explained as follows:

- During the sorption process, the adsorbate metal ions shift the adsorbed solvent molecules to have more translational entropy than the lost by the adsorbate, thus permitting randomness in the system [22].
- The positive value of $\Delta H°$ indicates that the sorption process is endothermic in nature. Decreasing in the $\Delta G°$ values shows the spontaneous and feasibility of adsorption process with increasing temperature [29].

4. Application

4.1. Breakthrough curves (column system)

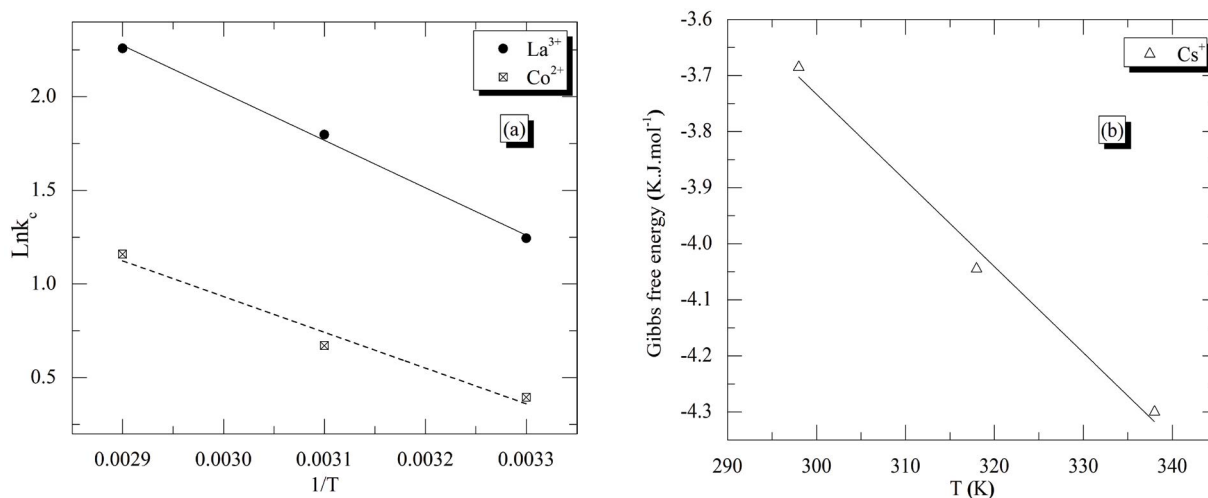Capacity and sorption isotherms obtained from the batch study do not give a perfect scale-up data for industrial

Fig. 5. Effect of temperature on the sorption of (a) both La^{3+} and Co^{2+} and (b) Cs$^+$ onto cellulose/HO$_7$Sb$_3$.

Table 6
Thermodynamic parameters for adsorption of La^{3+}, Co^{2+}, and Cs$^+$ ions on composite

Cation	Reaction temperature (K)	K_c	$\Delta H°$ (kJ mol^{-1})	$\Delta G°$ (kJ mol^{-1})	$\Delta S°$ (J mol^{-1} K^{-1})
La^{3+}	298	3.47	21.05	−2.48	0.079
	318	4.65		−4.06	
	338	8.66		−5.64	
Co^{2+}	298	1.50	15.80	−0.58	0.055
	318	2.08		−1.68	
	338	3.18		−2.79	
Cs$^+$	298	0.07	9.79	−3.78	0.015
	318	0.10		−4.17	
	338	0.14		−4.30	

systems, since sorption in a column is not usually in a state of equilibrium. Consequently, there is a need to make flow test using column prior to scale-up. Once working adsorption experiments through columns, the breakthrough curve (a plot of metal ion concentration in the effluent to the feed solution C/C_o vs. effluent volume V mL) is very beneficial. At 95% of effluent concentration, the column reaches to saturation (column exhaustion) [30]. To carry out the column experiment, a glass column of fixed bed depth = 5 cm was packed with 1.0 g of cellulose/HO$_7$Sb$_3$.

After conditioning the column with distilled water, La^{3+}, Co^{2+}, and Cs$^+$ solution with initial concentration of 100 mg L^{-1} passed through the column (flow rate = 5–6 drops per min). The resulted breakthrough curves are presented in Fig. 6. The values of breakthrough capacity for the studied cations can be evaluated from Fig. 6 and found to be 27.7, 25, and 20.5 mg g^{-1} for La^{3+}, Co^{2+}, and Cs$^+$, respectively

The elution outlines for La^{3+}, Co^{2+}, and Cs$^+$ ions are plotted in Fig. 7 for cellulose/HO$_7$Sb$_3$, the elution of these metal ions is studied in nitric acid solutions (0.01–0.5 M). Fig. 7 shows that, a large peak for La^{3+} ion is obtained and smaller peaks for Co^{2+} and Cs$^+$ at ≈90 mL of elution using 0.01 M HNO$_3$ followed by
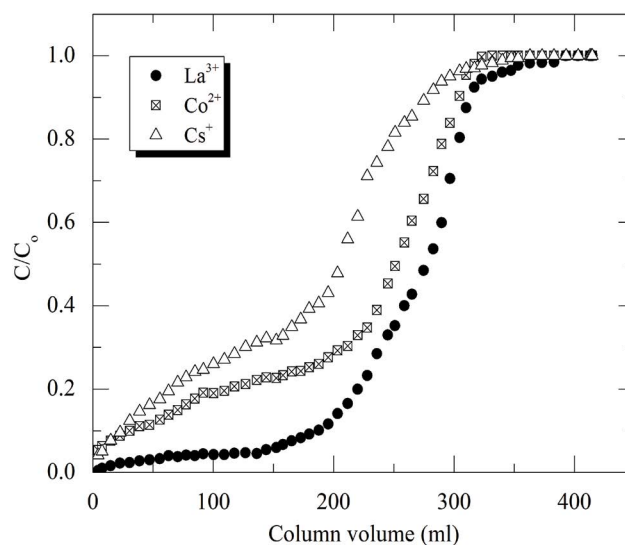

Fig. 6. Breakthrough curves of mixture of La^{3+}, Co^{2+}, and Cs$^+$ ions on cellulose/HO$_7$Sb$_3$ in pH = 5.5 and 25±1°C.
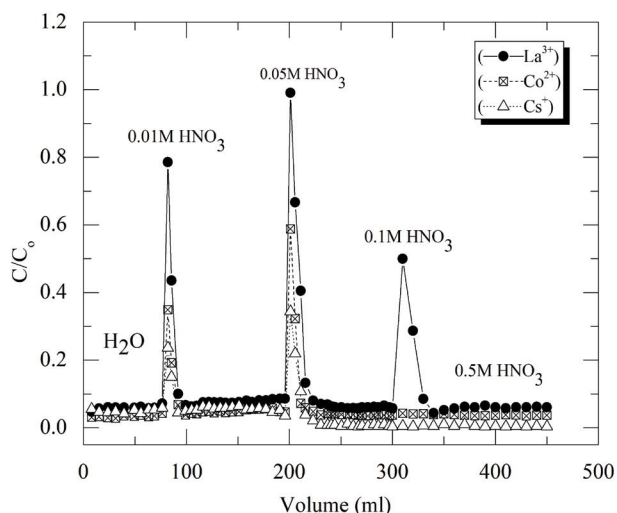
Fig. 7. Elution curves for the mixture of La³⁺, Co²⁺, and Cs⁺ with 0.01, 0.05, 0.1, and 0.5 M HNO₃ from cellulose/HO₇Sb₃ (0.5 cm diameter × 5 cm length and 5–6 drops min⁻¹ flow rate).

large peak for La³⁺, Co²⁺, and Cs⁺ at ≈210 mL elution using 0.05 M HNO₃ as a second eluent. At 0.1 M HNO₃, a large peak for La³⁺ at ≈310 mL elution and no peak for Co²⁺ and Cs⁺. So La³⁺ ions can be separated from the mixture of the studied metal ions using 0.1 M HNO₃. At 0.5 M HNO₃, no peaks were found and the adsorbed ions are almost completely removed (100%). Therefore, we can expect reusing the column after the regeneration process.

5. Conclusion

It is possible to conclude that cellulose/HO₇Sb₃ has high capacity for La³⁺, Co²⁺, and Cs⁺ at different pH and concentrations. From the applied kinetic models, the data are well fitted with pseudo-second-order model for all studied metal ions. In addition, the D–R isotherm model suggests the chemical adsorption behavior of sorption process for La³⁺ and Co²⁺. On the other hand, for Cs⁺ metal ion it is controlled by physical adsorption. The (+ve) value of $\Delta H°$ indicates that the sorption process is endothermic. The decrease in the $\Delta G°$ values indicates the spontaneous of sorption process. Finally, breakthrough curves show that the breakthrough capacity for La³⁺, Co²⁺, and Cs⁺ is 27.7, 25, and 20.5 mg g⁻¹ respectively. Additionally, cellulose/HO₇Sb₃ was employed to separate La³⁺ ions from La³⁺, Co²⁺, and Cs⁺ mixture using 0.1 M HNO₃. The optimum condition for column regeneration is to use 0.5 M HNO₃ removing all adsorbed metal ions.

References

[1] Y.F. El-Aryan, H. El-Said, E.A. Abdel-Galil, Synthesis and characterization of polyaniline-titanium tungstophosphate; Its analytical applications for sorption of Cs⁺, Co²⁺, and Eu³⁺ from waste solutions, Radiochemistry, 56 (2014) 614–621.

[2] E.A. Abdel-Galil, W.M. El-kenany, L.M.S. Hussin, Preparation of nanostructured hydrated antimony oxide using a sol-gel process. Characterization and applications for sorption of La³⁺ and Sm³⁺ from aqueous solutions, Russ. J. Appl. Chem., 88 (2015) 1351–1360.

[3] E.M. El Afifi, M.F. Attallah, E.H. Borai, Utilization of natural hematite as reactive barrier for immobilization of radionuclides from radioactive liquid waste, J. Environ. Radioact., 151 (2016) 156–165.

[4] M.S. Mansy, R.S. Hassan, Y.T. Selim, S.H. Kenawy, Evaluation of synthetic aluminum silicate modified by magnesia for the removal of ¹³⁷Cs, ⁶⁰Co and ¹⁵²⁺¹⁵⁴Eu from low-level radioactive waste, Appl. Radiat. Isot., 130 (2017) 198–205.

[5] M.M. Hamed, Sorbent extraction behavior of a nonionic surfactant, Triton X-100, onto commercial charcoal from low level radioactive waste, J. Radioanal. Nucl. Chem., 302 (2014) 303–313.

[6] H. Moloukhia, W.S. Hegazy, E.A. Abdel-Galil, S.S. Mahrous, Removal of Eu³⁺, Ce³⁺, Sr²⁺, and Cs⁺ ions from radioactive waste solutions by modified activated carbon prepared from coconut shells, Chem. Ecol., 32 (2016) 324–345.

[7] W. Plazinski, W. Rudzinski, A. Plazinska, Theoretical models of sorption kinetics including a surface reaction mechanism: a review, Adv. Colloid Interface Sci., 152 (2009) 2–13.

[8] E.A. Abdel-Galil, H. Moloukhia, M. Abdel-Khalik, S.S. Mahrous, Synthesis and physico-chemical characterization of cellulose/HO₇Sb₃ nanocomposite as adsorbent for the removal of some radionuclides from aqueous solutions, Appl. Radiat. Isot., 140 (2018) 363–373.

[9] M. Horsfall Jr, A.I. Spiff, Effects of temperature on the sorption of Pb²⁺ and Cd²⁺ from aqueous solution by *Caladium bicolor* (Wild Cocoyam) biomass, Electron. J. Biotechnol., 8 (2005) 162–169.

[10] E.A. Abdel-Galil, A.B. Ibrahim, M.M. Abou-Mesalam, Sorption behavior of some lanthanides on polyacrylamide stannic molybdophosphate as organic–inorganic composite, Int. J. Ind. Chem., 7 (2016) 231–240.

[11] B. El-Gammal, S.A. Shady, Chromatographic separation of sodium, cobalt and europium on the particles of zirconium molybdate and zirconium silicate ion exchangers, Colloids Surf., A, 287 (2006) 132–138.

[12] I.M. El-Naggar, E.A. Mowafy, G.M. Ibrahim, H.F. Aly, Sorption behaviour of molybdenum on different antimonates ion exchangers, Adsorption, 9 (2003) 331–336.

[13] A.K. El-Naggar, I.M. Mowafy, E.A., Abdel-Galil, E.A. Ghonaim, Adsorption of some hazardous radionuclides from their aqueous waste solutions using synthetic silico(IV)titanate, Arab J. Nucl. Sci. Appl., 41 (2008) 1–14.

[14] Y.S. Ho, J.C.Y. Ng, G. McKay, Kinetics of pollutant sorption by biosorbents: review, Sep. Purif. Methods, 29 (2000) 189–232.

[15] S. Lagergren, Zur theorie der sogenannten adsorption geloster stoffe, K. Sven. Vetens.akad. Handl., 24 (1898) 1–39.

[16] Y.S. Ho, G. Mckay, Pseudo-second order model for sorption processes, Process Biochem., 34 (1999) 451–465.

[17] Y.S. Ho, G. McKay, The kinetics of sorption of divalent metal ions onto sphagnum moss peat, Water Res., 34 (2000) 735–742.

[18] E.A. Abdel-Galil, H.E. Rizk, A.Z. Mostafa, Isotherm, kinetic, and thermodynamic studies for sorption of Cu(II) and Pb(II) by activated carbon prepared from *Leucaena* plant wastes, Part. Sci. Technol., 34 (2016) 540–551.

[19] L. Khezami, R. Capart, Removal of chromium(VI) from aqueous solution by activated carbons: kinetic and equilibrium studies, J. Hazard. Mater., 123 (2005) 223–231.

[20] E. Malkoc, Y. Nuhoglu, Potential of tea factory waste for chromium(VI) removal from aqueous solutions: thermodynamic and kinetic studies, Sep. Purif. Technol., 54 (2007) 291–298.

[21] W.J. Weber, J.C. Morris, Kinetics of adsorption on carbon from solution, J. Sanit. Eng. Div., 89 (1963) 31–60.

[22] F. Bouhamed, Z. Elouaer, J. Bouzid, B. Ouddane, Batch sorption of Pb(II) ions from aqueous solutions using activated carbon prepared from date stones: equilibrium, kinetic, and thermodynamic studies, 52 (2014) 2261–2271.

[23] V.J.P. Poots, G. McKay, J.J. Healy, The removal of acid dye from effluent using natural adsorbents—I peat, Water Res., 10 (1976) 1061–1066.

[24] I. Langmuir, The constitution and fundamental properties of solids and liquids. Part I. solids., J. Am. Chem. Soc., 38 (1916) 2221–2295.

[25] H.M. Freundlich, Over the adsorption in solution, J. Phys. Chem. A, 57 (1906) 385–470.

[26] B.P. Bering, M.M. Dubinin, V.V. Serpinsky, On thermodynamics of adsorption in micropores, J. Colloid Interface Sci., 38 (1972) 185–194.

[27] S. Sadeek, M.A. El-Sayed, M.M. Amine, M. Abd El-magied, A chelating resin containing trihydroxybenzoic acid as the functional group: Synthesis and adsorption behavior for Th(IV) and U(VI) ions, J. Radioanal. Nucl. Chem., 299 (2014) 1299–1306.

[28] Ö. Tunç, H. Tanacı, Z. Aksu, Potential use of cotton plant wastes for the removal of Remazol Black B reactive dye, J. Hazard. Mater., 163 (2009) 187–198.

[29] M. Kilic, E. Apaydin-Varol, A.E. Pütün, Adsorptive removal of phenol from aqueous solutions on activated carbon prepared from tobacco residues: equilibrium, kinetics and thermodynamics, J. Hazard. Mater., 189 (2011) 397–403.

[30] R. Ansari, Z. Mosayebzadeh, Removal of basic dye methylene blue from aqueous solutions using sawdust and sawdust coated with polypyrrole, J. Iran. Chem. Soc., 7 (2010) 339–350.